

# Solar radius measurements with the SODISM instrument : methods and algorithm developments for the PICARD Payload Data Center

A. Irbah<sup>1,\*</sup>, C. Dufour<sup>1</sup>, M. Meftah<sup>1</sup>, M. Meissonnier<sup>1</sup>, G. Thuillier<sup>1</sup>, P. Assus<sup>2</sup>, T. Corbard<sup>2</sup>, and G. Pradels<sup>3</sup>

<sup>1</sup> Université Versailles St-Quentin; CNRS/INSU, LATMOS-IPSL, Guyancourt, FRANCE

<sup>2</sup> Université de Nice Sophia-Antipolis, Laboratoire Cassiopée, Observatoire de la Côte d'Azur, BP 4229, 06304, Nice CEDEX 4, FRANCE

<sup>3</sup> CNES, Toulouse, 31401, FRANCE

**Key words** Sun: oscillations – Sun: general – Techniques: high angular resolution – Space vehicles: instruments

The PICARD space mission is scheduled for a launch in 2010. Its payload consists in 3 instruments: SODISM from LATMOS, SOVAP from IRMB (Belgium) and PREMOS from PMOD (Switzerland). SODISM key objective is to measure the diameter and shape of the Sun with an accuracy of a few milliarcseconds (mas), and their potential change during the increasing phase of the current solar cycle. We will present here some simulations and methods developed to make these measurements from SODISM images, and how these ones have been implemented at the PICARD Payload Data Center (PPDC) located at the B-USOC in Belgium.

© 2010 WILEY-VCH Verlag GmbH & Co. KGaA, Weinheim

## 1 Introduction

The solar diameter is measured since 3.5 centuries and its variation with the solar activity has been the subject of many researches. Data showed either variations in phase or antiphase with the solar activity or no variations. As the data were gathered from ground, the atmosphere was claimed to be responsible for the above inconsistencies. Very few observations outside the atmosphere exist showing variation from 30 to 400 milliarcseconds (mas). One of the primary objectives of the PICARD mission is to measure the solar diameter and shape with an accuracy of a few mas in orbit to avoid all atmospheric influence.

## 2 The SODISM instrument of the PICARD mission

The SODISM (Solar Diameter Imager and Surface Mapper) instrument makes an image of the Sun on a CCD detector. Wavelengths are selected by interference filters placed on 2 wheels. Wavelength domains are chosen free of Fraunhofer lines (535.7, 607 and 782 nm). Active regions are detected in the 215 nm domain and the CaII (393 nm) line. Helioseismic observations are performed at 535.7 nm. The satellite platform is stabilized at 36 arcseconds. The telescope primary mirror stabilizes the Sun image within 0.2 arcsecond using piezo electric actuators. An internal calibration system composed with 4 prisms, allows to follow scale factor variations induced by instrument deformations resulting from temperature fluctuations on orbit or others causes (Assus et al., 2008). The diameter measurements are referred

to star angular distances by rotating the spacecraft towards some doublet stars likely around every 3 months. The instrument stability is assured by use of stable materials : Zerodur for mirrors, Carbon-Carbon and Invar for structure. The whole instrument is temperature stabilized (1°C). The CCD is also temperature stabilized around -15°C within 0.2°C. In order to limit the solar energy, a window is set at the telescope entrance limiting the input to 5% of the TSI (Total Solar Irradiance). No significant ageing has been measured in laboratory for the duration of the mission. The optical scheme of SODISM is shown in Fig. 1.

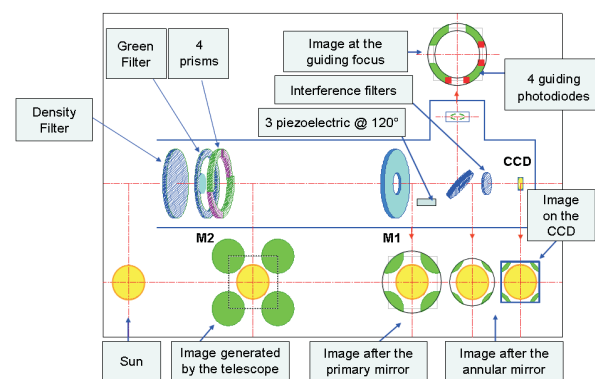


Fig. 1 SODISM optical scheme.

## 3 Numerical simulation - Expected results with SODISM

Numerical simulations were developed in order to study how changes of mechanical and optical instrumental prop-

\* Corresponding author: e-mail: air@latmos.ipsl.fr

erties affect SODISM images. Synthetic images were built for this goal using a numerical model of the solar limb darkening function. The SODISM optical scheme was implemented in the ZEMAX software. It allowed us to analyze geometrical properties of images but also to compute point spread functions (*psf's*) in several cases of interest. They consisted of moving positions of the primary and secondary mirrors and of the CCD camera focal plane. Image sampling effects on Sun radius measurements were also studied using synthetic and space images obtained with the MDI instrument of the SOHO satellite.

### 3.1 The solar limb and SODISM images

A numerical model was used to calculate the solar limb darkening function at the extremely solar edge (model computed by N. Mein, 2005). The center to limb intensity variation was computed using Hestrofer and Magnan's model (Hestrofer et al., 1998). This mixed model allowed us to build Sun images as they will be obtained with SODISM using *psf's* given by ZEMAX. A systematic displacement of the inflexion point of the limb is observed in the instrument focal plane. The figure 2 shows the limb darkening function and its derivative around the inflexion point. Solar radius will systematically be smaller than the true one with about 72 mas. Figure 3 show a simulated SODISM like image which will be used in the simulation to compute error on solar radius and instrument scale factors.

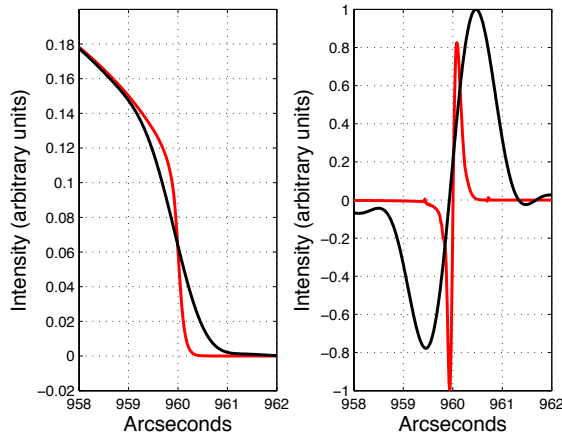


**Fig. 2** Limb darkening function model and its derivative. The theoretical mixed model is shown in red while the observed one in the SODISM focal plane is in black

### 3.2 The solar radius error

Solar radius measurements are affected when primary and secondary mirror positions move as well as the CCD focal plane one. A superposition of 2 effects on the SODISM images is then observed : a geometrical effect due to the

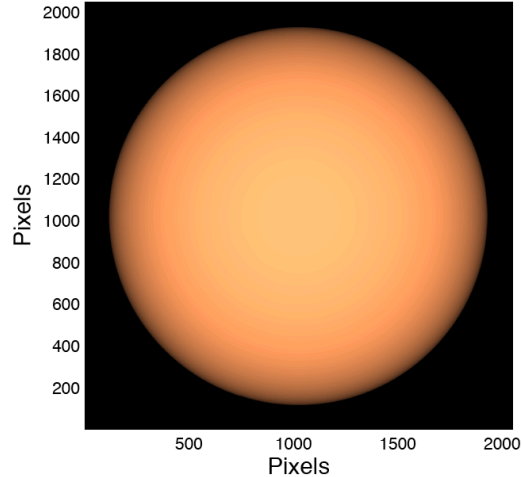


**Fig. 3** Simulated solar image as it will be obtained with SODISM.

SODISM design where its pupil image is at a finite distance and a diffraction one due to the limited pupil size. Table 1 resume the obtained results. They show that the optical diffraction effects are of second order compared to geometrical ones. The radius error is also negligible when the primary mirror is inclined to compensate from satellite platform vibrations. It is equal to about 0.25 mas when the mirror has its maximum allowed value (36 arcseconds) (see section 2).

**Table 1** Expected solar radius error obtained from simulations

SODISM ELEMENT	GEOMETRICAL ERROR	DIFFRACTION ERROR
Primary mirror	1 mas / 2.2 $\mu\text{m}$	1 mas / 0.01 $\mu\text{m}$
Secondary mirror	1 mas / 0.5 $\mu\text{m}$	1 mas / 0.02 $\mu\text{m}$
CCD focal plane	1 mas / 0.62 $\mu\text{m}$	1 mas / 0.001 $\mu\text{m}$

### 3.3 The image spatial sampling effects

The SODISM CCD camera has 2048x2048 square pixels. Their size is 13.5 mm width giving an angular image sampling of 1.06 arcseconds. This sampling will introduce an additional noise in the Sun radius values extracted from the images. In fact, Sun radius is defined as the inflexion point position of the solar limb darkening function which rise on less than 1 arcsecond. The sampling noise is more important in case of MDI images where the angular sampling is 1.96 arcseconds. We use here some MDI images adapted for the simulation. We have transformed them so as they have 2048x2048 pixel size. We have also added auxiliary images, a dark current recorded during SODISM tests and upgraded the pixel intensity to be coded on 15 bits (Fig. 4(a)). Figure 4(b) shows the solar radius  $\rho$  versus  $\theta$  extracted from a synthetic (blue) and a transformed MDI image (red and

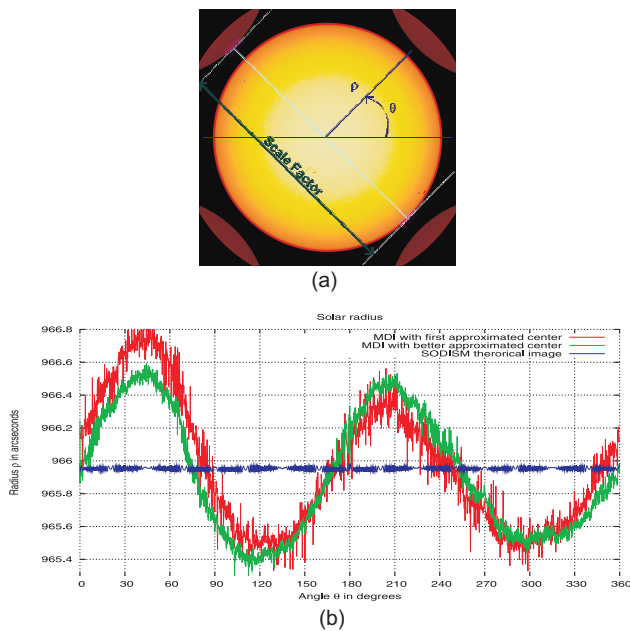


**Fig. 4** SODISM like image obtained from MDI ones (a) and its radius versus  $\theta$  in a polar coordinate system (b).

green). The red curve is obtained with a first order estimation of the image center. The green curve becomes near sinusoidal with a better center approximation, which corresponds to an ellipsoid fit with a 500 mas flattening. Noise standard deviation is equal to 40 and 10 mas for respectively the MDI and synthetic Sun images.

### 3.4 The SODISM scale factor

SODISM scale factor is monitored by mean of auxiliary images formed with the 4 prisms placed at the front of the instrument (see section 2). Several scale factor variations in synthetic images were given (Fig. 5). A poissonian noise and a SODISM dark current were added to the images. The method based on cross correlation properties was used (Assus et al., 2008). We were able in each case to retrieve scale factor input values with about 10 mas accuracy. It is the same value induced by the image sampling noise.

## 4 PICARD Payload Data Center : the PPDC

The PPDC (Pradels et al., 2008) will take in charge the programming of the payload, the processing of the acquisition data, the storage and the distribution of the PICARD scientific products. The PPDC will create the three data levels L0, L1 and L2A. All kinds of the SODISM L0 products are shown in figure 6. They were obtained during SODISM tests or from simulations. Quick-look analysis on L0 and L1 products will also generate some products at the PPDC.

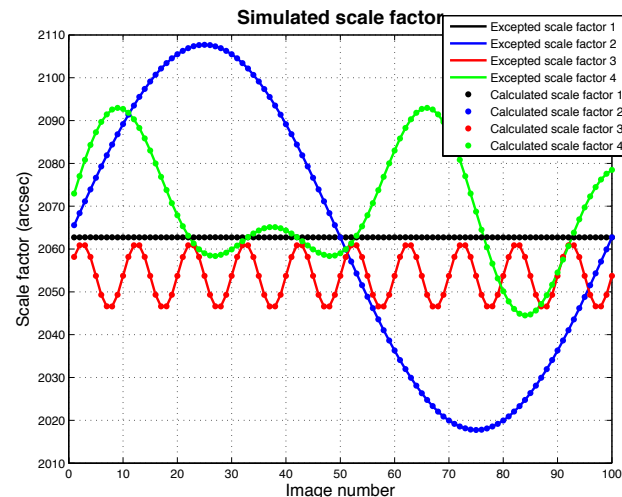


**Fig. 5** Estimation of SODISM scale factor.

## 4.1 The SODISM data

### 4.1.1 Full solar images

Full solar images are 2048x2048 and 256x256 pixels size. The first kind of images will be recorded at all PICARD wavelengths with a cadence of 2 of them per orbit while the others will be recorded each minute at 535.7 nm.

### 4.1.2 Solar and dark signal limb images

Limb images are 2048x2048 pixels size and correspond to 22 and 40 pixels wide limbs. They will be recorded respectively at the wavelength 535.7 nm each 2 minutes and at all PICARD wavelengths with a rate of 2 per orbit. Dark signal limb image is 40 pixels wide. Several markers (dark signal and scattered light) extracted from the full CCD image are presents with the limb (see section 4.2.1). The 4 auxiliary images are also but only presents at 535.7 nm.

### 4.1.3 Others data

These data are images of doublet stars field, dark signal and flat field at 215, 535.7, 607 and 782 nm obtained by mean of a divergent lens. An image of a dark signal and a flat field at a given wavelength will be recorded every day while a sequence of doublet stars field images every 3 months. All image sizes at PPDC are 2048x2048 pixels.

## 4.2 Scientific algorithms

We need to know how the data are processed onboard to understand algorithms which will be implemented in the PPDC to create L0 products. Onboard data processing concern principally SODISM images. This is due to the large volume of data generated by the instrument relatively to the allowed transmission rate.

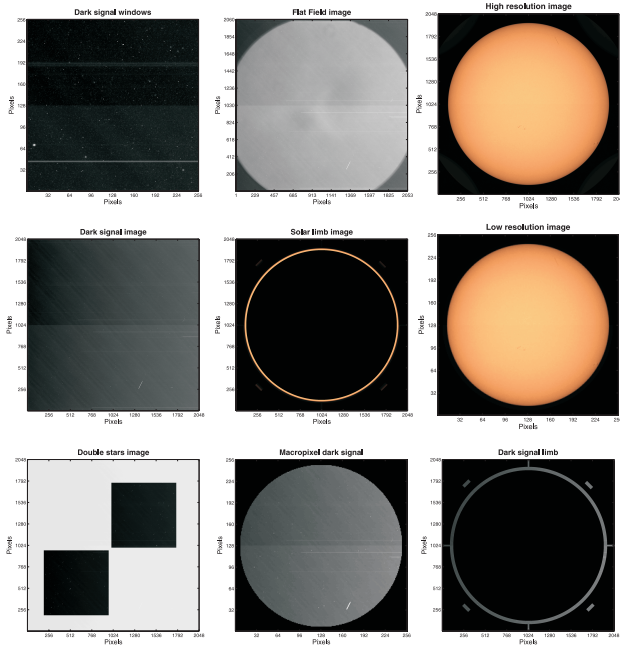


**Fig. 6** All kinds of L0 SODISM products

#### 4.2.1 Onboard data processing

Limb images are extracted applying a mask on SODISM images. It is built so as to acquire also auxiliary images and markers (Fig. 7). A transformation of the limb image is made to keep only non-zero pixels which are projected on the y-axis. The transformed limb is related to the used mask (Fig. 7). The other onboard data processing allows generating solar full images made of macro-pixels. They are obtained by convolving SODISM images with a chosen spatial window. The macro-pixel image has after that a size of 256x256 pixels. The last onboard data processing is a compression operation. Two kinds of compression are used. The first one is a lossless compression for transformed limbs, macro-pixel solar images and some others images (flat field, dark signal and doublet stars field). The second kind is a destructive compression used for some solar images. The degradation factor is chosen so as to not affect scientific objectives. All scientific data are divided into packets. Others packets containing housekeeping data and image parameters are added before sending the whole by telemetry.

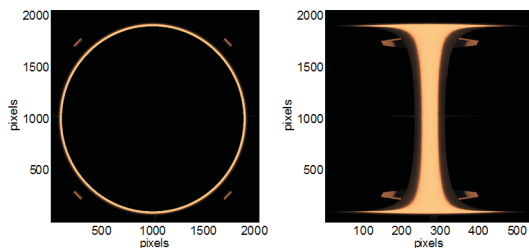


**Fig. 7** Solar limb (right) and its onboard transformation (left)

#### 4.2.2 SODISM data processing

We present now the scientific software used to create PPDC products, which are all FITS format.

*a* – Level 0 and quick-look L0’: The first step to create L0 products is to assemble the data packets and to generate the binary stream. The next one is to decompress it if needed, before it will be the appropriate software input. All full images products are then built (macro-pixels, dark signal, flat field and stars field) adding for that housekeeping data in their header. The inverse transformation made on-board is necessary before creating limb products. All markers presents in the solar limbs are extracted to form daily L0 products. Quick-look analysis is made on daily marker products and dark signal full image. It consists in computing the mean and standard deviation of pixel intensity but also to count and locate the bad pixels in the images.

*b* – Level 1 and quick-look L1’: The Level 1 processing sequences consist in L0 product calibration and to add information in their header. They consist also to create daily products containing the auxiliary images. Others processing sequences are implemented to monitor the limb and macro-pixel image intensity.  $l\nu$  diagram is also computed every 3 days as quick-look using macro-pixel images. Another quick-look is the calculation every 15 days of the temporal fluctuation power spectrum of 22 pixels wide limb and macro-pixel image intensity. The last quick-look is an intensity analysis of the full images recorded at all PICARD wavelengths. It is then compared with PREMOS data.

*c* – Level 2A : The level 2 processing sequences consist in computing the mean solar radius from each limb image and its daily variations. Measurement accuracy and polluting noise are also estimated. L2A products are enriched every day and unique for the entire space mission duration.

## 5 Conclusion

The SODISM instrument has been developed for solar astrometry and helioseismology observations. Some simulations have been made to well understand the measurement errors due to instrument deformations in orbit. Synthetic and transformed MDI solar images have been used for that. They also allows us to test how to compute the SODISM scale factor. The developed methods deduced from the simulations, will be implemented in the PICARD Payload Data Center. An overview of the PPDC has been then given as well as the SODISM products that will be created there.

## References

- Assus, A., Irbah, A., Bourget P., Corbard T., and the PICARD team : 2008, Astron. Nachr. 329, No. 5, 517 - 520
- Mein, N.: 2005, LESIA, private communication
- Hestroffer, D., Magnan, C., and Loeser, R.: 1998, Astronomy and Astrophysics, v.333, p.338-342
- Pradels, G. et al., SPACEOPS 2008 conference